VI International Conference on Computational Methods for Coupled Problems in Science and Engineering
COUPLED PROBLEMS 2015
B. Schrefler, E. Oñate and M. Papadrakakis(Eds)

THE EFFICIENCY COMPARISON OF THE VORTEX ELEMENT METHOD AND THE IMMERSED BOUNDARY METHOD FOR NUMERICAL SIMULATION OF AIRFOIL'S HYDROELASTIC OSCILLATIONS

ILIA K. MARCHEVSKY, VICTORIYA S. MOREVA AND VALERIA V. PUZIKOVA

Bauman Moscow State Technical University (BMSTU)
Applied Mathematics department
Russia, 105005 Moscow, 2nd Baumanskaya, 5
e-mail: iliamarchevsky@mail.ru, morevavs@rambler.ru, valeria.puzikova@gmail.com

Key words: Vortex Element Method, Immersed Boundary Methods, The LS-STAG Method, Coupled Hydroelastic Problems, Wind Resonance

Abstract. In the present research the well-known test problem of wind resonance phenomenon simulation is considered. The Vortex Element Method and the LS-STAG method are used for its solving and their comparison is carried out. The obtained results can be useful for scientists and engineers who develop and operate the constructions which structural elements oscillate under hydrodynamic forces.

1 INTRODUCTION

Lagrangian meshless Vortex Element Methods [1, 2] are well-known numerical methods which efficiency can be very high when solving coupled aerohydroelastic problems. They allow to simulate both viscous and inviscid incompressible flows in bounded and unbounded domains. Vortex Element Methods for 2D flows are well developed and there are number of approaches for viscosity accounting (e.g., Viscous Vortex Domains method [3]) and for boundary conditions satisfaction. The main advantage of Vortex Element Method is that there is no necessity of mesh constructing and reconstructing when the airfoil moves and the airfoil can be of arbitrary shape. It also provides small numerical viscosity and requires sufficiently small memory and time of computations.

For flow simulation around airfoils with complicated shape or when the Reynolds number is about tens of thousands the number of vortex elements should be very large to provide the necessary accuracy. There are some approaches for accuracy improvement [4], mainly based on the modified mathematical models, an also number of approaches for

computations speedup, which presuppose parallel computational algorithms and fast approximate multipole methods usage. These approaches allow to simulate unsteady flows and to solve directly coupled hydroelastic problems even on personal computers.

Another effective method for coupled hydroelastic problems solving which also doesn't require mesh reconstruction is Immersed Boundary Method [5]. Its LS-STAG [6] modification is one of the most accurate algorithms because it provides correct approximation of the governing equations both on rectangular fluid cells and cut-cells. Because of rectangular mesh usage the uniform 5-point stencil inside the flow region and 4 or 3-point stencils at the boundaries are used, so it is possible to use high-efficiency numerical methods (e.g. Krylov subspaces, multigrid preconditioners etc.) for linear systems solving. RANS-based turbulence models have been recently implemented to LS-STAG method, so it can be used in coupled problems when the Reynolds number is about tens of thousands.

In the present research the well-known test problem of wind resonance phenomenon simulation is considered. The Vortex Element Method and the LS-STAG method are used for its solving and their comparison is carried out.

2 GOVERNING EQUATIONS

The problem is considered in 2D unsteady case when the flow around an airfoil is viscous and incompressible. The continuity and momentum equations are the following:

$$\nabla \cdot \vec{V} = 0, \qquad \frac{\partial \vec{V}}{\partial t} + (\vec{V} \cdot \nabla)\vec{V} = \nabla p + \frac{1}{\mathrm{Re}}\Delta \vec{V}. \tag{1}$$

Here $\vec{V} = \vec{V}(x, y, t) = u \cdot \vec{e}_x + v \cdot \vec{e}_y$ is the dimensionless velocity, $p = p(x, y, t)$ is the dimensionless pressure. The boundary conditions are the following:

$$\vec{V}\big|_{\text{inlet}} = \vec{V}_\infty, \qquad \frac{\partial \vec{V}}{\partial \vec{n}}\Big|_{\text{outlet}} = 0, \qquad \frac{\partial p}{\partial \vec{n}}\Big|_{\text{inlet\&outlet}} = 0, \tag{2}$$

$$\vec{V}\big|_{\text{airfoil}} = \vec{V}^{\,\text{ib}}, \qquad \frac{\partial p}{\partial \vec{n}}\Big|_{\text{airfoil}} = 0. \tag{3}$$

Here $\vec{V}^{\text{ib}}$ is the velocity of the immersed boundary. The airfoil is assumed to be rigid.

To simulate wind resonance phenomenon we consider the motion of the circular airfoil with diameter D across the stream (with one degree of freedom). Airfoil's constrain assumed to be linear viscoelastic Kelvin — Voigt-type (fig. 1) and its motion is described by the following ordinary differential equation:

$$m\ddot{y}_* + b\dot{y}_* + ky_* = F_y. \tag{4}$$

Here m is the airfoil mass, b is small damping factor, k is the constraint's elasticity coefficient, F_y is lift force, y_* is the deviation from the equilibrium. The natural frequency of the system $\omega \approx \sqrt{k/m}$ can be changed by varying of the coefficient k.

The deviation from the equilibrium on the n-th step of computation is $y_*^n = Y_C^n - Y_C^0$. Here Y_C^0 is the ordinate of the airfoil center at the initial time and Y_C^n is the ordinate of the airfoil center at the n-th step of computation.

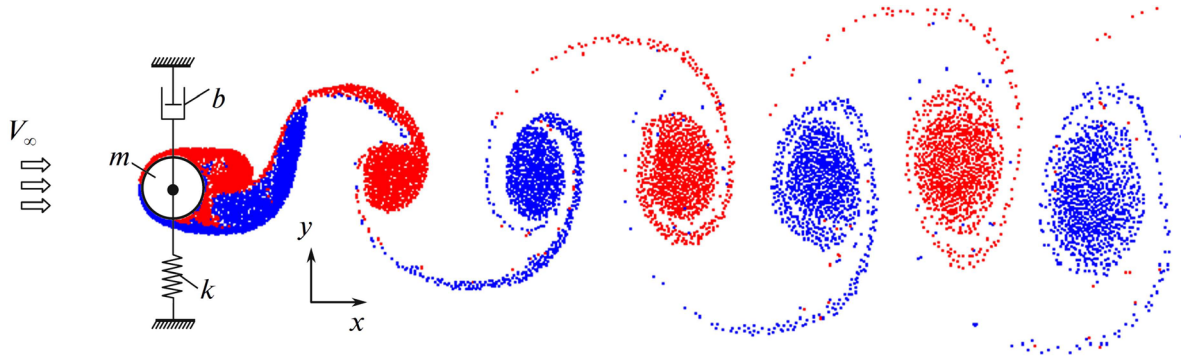

Figure 1: The circular airfoil with Kelvin — Voigt viscoelastic constraint and vortex wake behind it

In all numerical simulations with the following values of dimensionless parameters have been chosen: $\mathrm{Re} = 1000$, $V_\infty = 3.0$, $m = 39.15$, $b = 0.731$. The dimensionless natural frequency of the system is in the following range:

$$\mathrm{Sh}_\omega = \frac{\omega}{2\pi} \cdot \frac{D}{V_\infty} = 0.150 \ldots 0.280. \tag{5}$$

3 MAIN IDEAS OF THE VORTEX ELEMENT METHOD

Navier — Stokes equations (1) could be written down in Helmholtz form using vorticity vector $\vec{\Omega}(\vec{r},\, t) = \nabla \times \vec{V}(\vec{r},\, t)$:

$$\frac{\partial \vec{\Omega}}{\partial t} + \nabla \times (\vec{\Omega} \times \vec{U}) = 0. \tag{6}$$

Here $\vec{U}(\vec{r}, t) = \vec{V}(\vec{r}, t) + \vec{W}(\vec{r}, t)$, $\vec{W}(\vec{r}, t)$ is the so-called diffusive velocity [3], which is proportional to viscosity coefficient:

$$\vec{W}(\vec{r}, t) = \nu \frac{(\nabla \times \vec{\Omega}) \times \vec{\Omega}}{|\vec{\Omega}|^2}. \tag{7}$$

If vorticity distribution is known, flow velocity can be computed using Biot — Savart law:

$$\vec{V}(\vec{r}) = \vec{V}_\infty + \frac{1}{2\pi} \int_S \frac{\vec{\Omega}(\vec{\xi}, t) \times (\vec{r} - \vec{\xi})}{|\vec{r} - \vec{\xi}|^2} dS. \tag{8}$$

Equation (6) means that vorticity in the flow moves and its velocity is $\vec{U}$. 'New' vorticity is being generated only on airfoil surface ant this vortex layer intensity can be found from boundary condition of airfoil surface.

Vortex element method is meshless particle-type methods, so the vorticity field in the flow is discretized into separate vortex elements. Each vortex element is described by its position $\vec{r}_i$ and circulation Γ_i, $i = 1, \ldots, N$, where N is number of vortex elements in the flow. So the discretized Biot — Savar law has the following form:

$$\vec{V}(\vec{r}) = \vec{V}_\infty + \sum_{i=1}^{N} \frac{\Gamma_i}{2\pi} \frac{\vec{k} \times (\vec{r} - \vec{r}_i)}{|\vec{r} - \vec{r}_i|^2} + \oint_K \frac{\vec{k} \times (\vec{r} - \vec{\xi})}{2\pi |\vec{r} - \vec{\xi}|^2} \gamma(\vec{\xi})\, dl_\xi. \tag{9}$$

Here $\vec{k}$ is unit vector of the axis which is orthogonal to the plane of the flow.

Vortex elements movement according to (6) is simulated via solving the following ordinary differential equations system:

$$\frac{d\vec{r}_i}{dt} = \vec{V}(\vec{r}_i) + \vec{W}(\vec{r}_i), \quad i = 1, \ldots, N. \tag{10}$$

Number of vortex elements in the flow N changes at every time step because of the vorticity flux from the airfoil surface, which is simulated by vortex element generation near the airfoil. Their circulations are calculated from the vortex layer intensity $\gamma(\vec{\xi})$ on the airfoil surface. The circulations of all vortex elements in the flow remain constant and they can change only in special numerical procedure of vortex wake restructuring which allows to merge closely spaced vortex elements and lower their number in the flow.

Vortex layer intensity $\gamma(\vec{\xi})$ is unknown and can be found from the boundary condition

$$\vec{V}_-(\vec{r}) = \vec{V}^{\,\mathrm{ib}}(\vec{r}), \quad \vec{r} \in K. \tag{11}$$

Here $\vec{V}_-(\vec{r})$ is limit value of velocity from the airfoil side,

$$\vec{V}_-(\vec{r}) = \vec{V}_\infty + \sum_{i=1}^{N} \frac{\Gamma_i}{2\pi} \frac{\vec{k} \times (\vec{r} - \vec{r}_i)}{|\vec{r} - \vec{r}_i|^2} + \oint_K \frac{\vec{k} \times (\vec{r} - \vec{\xi})}{2\pi |\vec{r} - \vec{\xi}|^2} \gamma(\vec{\xi})\, dl_\xi - \frac{\gamma(\vec{r})}{2} \left(\vec{k} \times \vec{n}(\vec{r})\right) \tag{12}$$

$\vec{n}(\vec{r})$ is unit normal vector on the airfoil surface in point $\vec{r}$.

It can be shown [7] that we can solve one of scalar equation

$$\vec{V}_-(\vec{r}) \cdot \vec{n}(\vec{r}) = \vec{V}^{\,\mathrm{ib}}(\vec{r}) \cdot \vec{n}(\vec{r}) \qquad \text{or} \qquad \vec{V}_-(\vec{r}) \cdot \vec{\tau}(\vec{r}) = \vec{V}^{\,\mathrm{ib}}(\vec{r}) \cdot \vec{\tau}(\vec{r}) \tag{13}$$

instead of vector equation (11). Here $\vec{\tau}(\vec{r})$ is unit tangent vector on the airfoil surface. Mathematically there is no difference between solutions of these equations, but from computational point of view the corresponding numerical schemes are very different.

In 'classical' approach [1, 2, 3] unknown vortex layer intensity on the airfoil surface is assumed to be piecewise constant function and it satisfies equation $\vec{V}_- \cdot \vec{n} = \vec{V}^{\,\mathrm{ib}} \cdot \vec{n}$, which corresponds to equality of the flow and airfoil's velocity normal components on the airfoil surface and leads to singular integral equation of the 1-st kind

$$\oint_K \frac{\left[\vec{k} \times (\vec{r} - \vec{r}_0)\right] \cdot \vec{n}(\vec{r})}{2\pi |\vec{r} - \vec{r}_0|^2} \gamma(\vec{r}_0)\, dl_{r_0} = -\vec{n}(\vec{r}) \cdot \left(\vec{V}_\infty - \vec{V}^{\,\mathrm{ib}}(\vec{r}) + \sum_{i=1}^{N} \frac{\Gamma_i}{2\pi} \frac{\vec{k} \times (\vec{r} - \vec{r}_i)}{|\vec{r} - \vec{r}_i|^2} \right). \tag{14}$$

The solution of (14) certainly exists due to form of right side of this equation, but it is not unique. In order to select the unique solution an additional condition should be added:

$$\oint_K \gamma(\vec{r}) dl_r = G. \tag{15}$$

The kernel of equation (14) is unbounded and it has nonintegrable Hilbert-type singularity when $|\vec{r}-\vec{r}_0| \to 0$, so special numerical schemes are used for Cauchy principal value computation. They allow to obtain the solution of linear system approximating (14) with high accuracy when number of collocating points on the airfoil is large and its surface is smooth curve. It is proved [1] that in this case numerical solution converges to exact one in some integral (Hölder) norm. This approach lies in the basis of the 'classical' method; it can be called 'NVEM' — Vortex Element Method with normal components of velocity on airfoil surface.

The well-known numerical schemes [1], which are effective in vortex element method for inviscous fluids, can be generalized for viscous case, but the difference between numerical and exact solutions in uniform norm sometimes becomes significant. In order to take into account correctly the influence of the term with sum in the right side we need to discretize the airfoil extremely precisely, but it will lead to linear system with inadmissibly big dimension which coefficients and right side computation as well as solution have a very big computation cost.

At the same time if we simulate flow around the airfoil with angle points or sharp edges using NVEM, the error sometimes even increases proportionally to number of collocating points on the airfoil surface [4, 8]. So it is impossible to determine the vortex layer intensity with high accuracy and classical NVEM-schemes can't be applied for 2D Navier — Stockes equations solution for airfoils with angle points and sharp edges. The matrix of the linear system also can be ill-conditioned.

It also should be noted that linear algebraic system corresponding to (14) becomes ill-conditioned for airfoils with angle points or sharp edges.

In order to solve the mentioned problems, the alternative approach based on ideas [7] is developed by the authors [4, 8]. Vortex layer intensity is determined from solution of equation $\vec{V}_- \cdot \vec{\tau} = \vec{V}^{\,\mathrm{ib}} \cdot \vec{\tau}$, corresponding to equality of tangent component of flow velocity limit value and airfoil surface velocity. It leads to Fredholm-type integral equation of the 2-nd kind with bounded (for smooth airfoils) kernel:

$$\oint_K \frac{\left[\vec{k} \times (\vec{r}-\vec{r}_0)\right] \cdot \vec{\tau}(\vec{r})}{2\pi|\vec{r}-\vec{r}_0|^2} \gamma(\vec{r}_0) dl_{r_0} - \frac{\gamma(\vec{r})}{2} = -\vec{\tau}(\vec{r}) \cdot \left(\vec{V}_\infty - \vec{V}^{\,\mathrm{ib}}(\vec{r}) + \sum_{i=1}^{N} \frac{\Gamma_i}{2\pi} \frac{\vec{k} \times (\vec{r}-\vec{r}_i)}{|\vec{r}-\vec{r}_i|^2} \right). \tag{16}$$

Solution of equation (16) is also non-unique, so the same additional condition (15) as in classical method is used. This method is called 'TVEM' — Vortex Element Method with tangent components of velocity on airfoil surface.

Equation (16) also can be approximated with linear algebraic system which is well-conditioned both for smooth and non-smooth airfoils. Due to equation kernel boundness an arbitrary quadrature formula can be used for integral approximation in (16). In simplest case we also can consider vortex layer intensity to be piecewise constant function.

Results of numerical experiments show that errors are sufficiently big, but they could be significantly decreased if we consider some 'weak' formulation of (16): integral equa-

tion (16) in discrete numerical scheme will be satisfied not in separate collocation points $\vec{r}_j$, $j = 1, \ldots, N$ of airfoil surface, but on an average on airfoil surface parts (panels) K_p whose lengthes are L_p, $p = 1, \ldots, N$:

$$\frac{1}{L_p}\int_{K_p}\left[\oint_K \frac{\left[\vec{k}\times(\vec{r}-\vec{r}_0)\right]\cdot\vec{\tau}(\vec{r})}{2\pi|\vec{r}-\vec{r}_0|^2}\gamma(\vec{r}_0)dl_{r_0}\right]dl_r - \frac{1}{L_p}\int_{K_p}\frac{\gamma(\vec{r})}{2}dl_r =$$

$$= -\frac{1}{L_p}\int_{K_p}\vec{\tau}(\vec{r})\cdot\left(\vec{V}_\infty - \vec{V}^{\,\mathrm{ib}}(\vec{r})\right)dl_r - \frac{1}{L_p}\sum_{i=1}^{N}\frac{\Gamma_i}{2\pi}\int_{K_p}\frac{\vec{k}\times(\vec{r}-\vec{r}_i)}{|\vec{r}-\vec{r}_i|^2}dl_r, \quad p = 1, \ldots, N. \quad (17)$$

The other modification concerns uniform vorticity distribution on airfoil surface. In 'classical' NVEM method intensity of vortex layer assumed to be constant on every part (every panel) of the airfoil, but then all the vorticity from every panel concentrates in one point on the panel and integral in (14) transforms into a sum of influences of discrete (point) vortex elements. In the developed modified method TVEM vorticity assumed to be uniformly distributed over every panel. Every panel on the airfoil is straight-line segment, so internal integral in first term (17) transforms into a sum of influences of panels with uniformly distributed vorticity which intensity on the q-th panel is equal to γ_q:

$$\sum_{q=1}^{N}\frac{\gamma_q}{L_p}\int_{K_p}\left[\int_{K_q}\frac{\left[\vec{k}\times(\vec{r}-\vec{r}_0)\right]\cdot\vec{\tau}(\vec{r})}{2\pi|\vec{r}-\vec{r}_0|^2}dl_{r_0}\right]dl_r - \frac{\gamma_p}{2} =$$

$$= -\frac{1}{L_p}\int_{K_p}\vec{\tau}(\vec{r})\cdot\left(\vec{V}_\infty - \vec{V}^{\,\mathrm{ib}}(\vec{r})\right)dl_r - \frac{1}{L_p}\sum_{i=1}^{N}\frac{\Gamma_i}{2\pi}\int_{K_p}\frac{\vec{k}\times(\vec{r}-\vec{r}_i)}{|\vec{r}-\vec{r}_i|^2}dl_r, \quad p = 1, \ldots, N. \quad (18)$$

All the integrals in (18) can be calculated analytically, the corresponding formulae are derived in [4, 8]. Numerical results show that the developed TVEM-scheme and especially its 'weak' form allows to increase the accuracy significantly: sometimes the error becomes a tens or even hundreds times smaller [4, 8].

In order to compute the pressure distribution and hydrodynamic force which effect on the airflow, the analogues of Bernoulli and Cauchy — Lagrange integrals are used [9]. This approach is very effective in Vortex Element method and it can be equally applied for both NVEM and TVEM schemes.

It should be noted that computation cost of simulating fixed and movable rigid airfoils when using vortex element method remains nearly the same, so they are very suitable for coupled aerohydroelastic problems. However vortex element movement simulation is 'N-body'-type problem, and in practice number of vortex element can be on the order of tens and sometimes even hundreds of thousand, so special acceleration algorithms should be implemented. Well-known Barnes — Hut fast algorithm analogue [10] can be very effective, especially when using accurate analytical estimate of its computational cost [11] which allows to choose its parameters optimally. Parallel computation algorithms are also used in order to reduce time of computations [12].

4 MAIN IDEAS OF THE LS-STAG METHOD

The Cartesian mesh with cells $\Omega_{i,j} = (x_{i-1}, x_i) \times (y_{j-1}, y_j)$ is introduced in the rectangular computational domain. It is denoted that $\Gamma_{i,j}$ is the face of $\Omega_{i,j}$ and $\vec{x}^c_{i,j} = (x^c_i, y^c_j)$ is the center of this cell. Unknown components $u_{i,j}$ and $v_{i,j}$ of velocity vector $\vec{v}$ are computed in the middle of fluid parts of the cell faces. These points are the centers of control volumes $\Omega^u_{i,j} = (x^c_i, x^c_{i+1}) \times (y_{j-1}, y_j)$ and $\Omega^v_{i,j} = (x_{i-1}, x_i) \times (y^c_j, y^c_{j+1})$ with faces $\Gamma^u_{i,j}$ and $\Gamma^v_{i,j}$ and areas M^x_{ij} and $M^y_{i,j}$ respectively (fig. 2). If $i = \overline{1, N}$, $j = \overline{1, M}$, base mesh, x-mesh and y-mesh contain $E = N \cdot M$, $E_x = (N-1) \cdot M$ and $E_y = N \cdot (M-1)$ cells correspondingly.

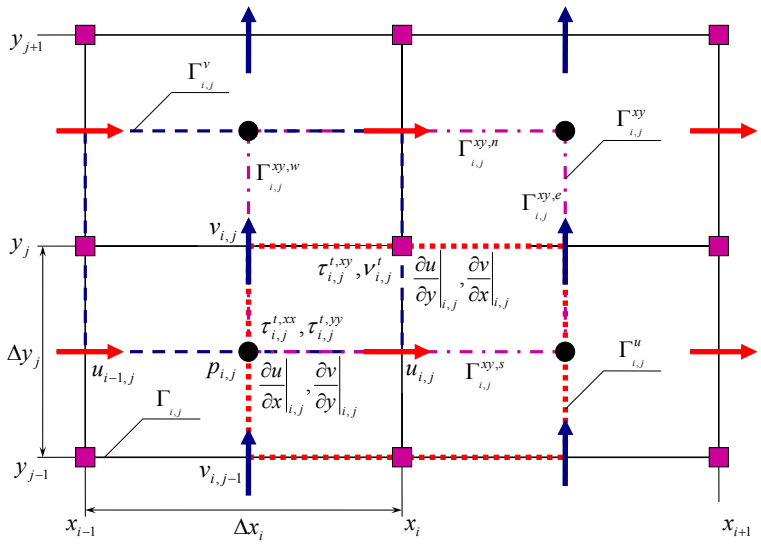

Figure 2: Staggered arrangement of the variables on the LS-STAG mesh

The level-set function $\varphi = \varphi(x, y)$ [13] is used for immersed boundary Γ^{ib} description [6]. Cells which the immersed boundary intersects are the so-called 'cut-cells' (fig. 3). These cells contain the solid part together with the liquid one. The boundary Γ^{ib} is represented by a line segment on the cut-cell $\Omega_{i,j}$. Location of this segment endpoints are defined by a linear interpolation of the variable $\varphi_{i,j} = \varphi(x_i, y_j)$.

The cell-face fraction ratios $\vartheta^u_{i,j}$ and $\vartheta^v_{i,j}$ are introduced in [6]. They take values in interval $[0, 1]$ and represent the fluid parts of the east and north faces of $\Gamma_{i,j}$ respectively. One-dimensional linear interpolation of $\varphi(x_i, y)$ on the segment $[y_{j-1}, y_j]$ and $\varphi(x, y_j)$ on the segment $[x_{i-1}, x_i]$ is used for the cell-face fraction ratios computing:

$$\vartheta^u_{i,j} = \frac{\min(\varphi_{i,j-1}, \varphi_{i,j})}{\min(\varphi_{i,j-1}, \varphi_{i,j}) - \max(\varphi_{i,j-1}, \varphi_{i,j})}, \quad \vartheta^v_{i,j} = \frac{\min(\varphi_{i-1,j}, \varphi_{i,j})}{\min(\varphi_{i-1,j}, \varphi_{i,j}) - \max(\varphi_{i-1,j}, \varphi_{i,j})}. \quad (19)$$

In 2D case, the cut-cells can be classified into trapezoidal, triangular and pentagonal cells. Examples of each type cut-cells are presented on fig. 3.

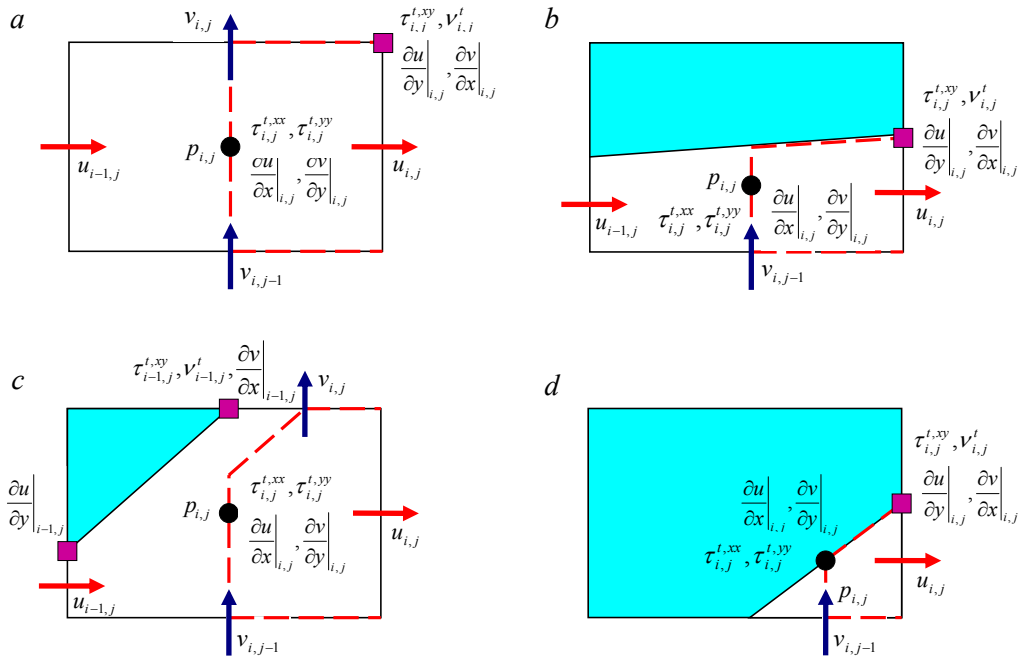

Figure 3: Location of the variables discretization points on the LS-STAG mesh: a – Cartesian Fluid Cell; b – North Trapezoidal Cell; c – Northwest Pentagonal Cell; d – Northwest Triangle Cell.

To preserve the five-point structure of the stencil of the MAC method we need to make distinction between the discretization of the normal and shear stresses (fig. 3).

Hydrodynamic force can be computed by the following formulae:

$$F_x = \sum_{\text{Cut-cells } \Omega^{ib}_{i,j}} \left[(\vartheta^u_{i-1,j} - \vartheta^u_{i,j}) \Delta y_j \left(p_{i,j} - \nu \frac{\partial u}{\partial x}\Big|_{i,j} \right) - \nu \text{Quad}^{ib}_{i,j} \left(\frac{\partial u}{\partial y} \vec{e}_y \cdot \vec{n} \right) \right], \tag{20}$$

$$F_y = \sum_{\text{Cut-cells } \Omega^{ib}_{i,j}} \left[-\nu \text{Quad}^{ib}_{i,j} \left(\frac{\partial v}{\partial x} \vec{e}_x \cdot \vec{n} \right) + (\vartheta^v_{i,j-1} - \vartheta^v_{i,j}) \Delta x_i \left(p_{i,j} - \nu \frac{\partial v}{\partial y}\Big|_{i,j} \right) \right].$$

The quadrature of the shear stresses $\text{Quad}^{ib}_{i,j}$ has to be adapted to each type of cut-cells.

According to the concept of the LS-STAG method equations (1) should be written in integral form for cell of base mesh, cell of x-mesh and cell of y-mesh respectively:

$$\int_{\Gamma_{i,j}} \vec{v} \cdot \vec{n} \, dS = 0, \tag{21}$$

$$\frac{d}{dt} \int_{\Omega^u_{i,j}} u \, dV + \int_{\Gamma^u_{i,j}} (\vec{v} \cdot \vec{n}) u \, dS + \int_{\Gamma^u_{i,j}} p \vec{e_x} \cdot \vec{n} \, dS - \int_{\Gamma^u_{i,j}} \nu \nabla u \cdot \vec{n} \, dS = 0,$$

$$\frac{d}{dt} \int_{\Omega^v_{i,j}} v \, dV + \int_{\Gamma^v_{i,j}} (\vec{v} \cdot \vec{n}) v \, dS + \int_{\Gamma^v_{i,j}} p \vec{e_y} \cdot \vec{n} \, dS - \int_{\Gamma^v_{i,j}} \nu \nabla v \cdot \vec{n} \, dS = 0.$$

The general form of the LS-STAG discretization for (21) is the following [6]:

$$D^x U_x + D^y U_y + \overline{U}^{ib} = 0, \tag{22}$$
$$\frac{d}{dt}(M^x U_x) + C^x U_x + G^x P - \nu K^x U_x + S_x^{ib,c} - \nu S_x^{ib,\nu} = 0,$$
$$\frac{d}{dt}(M^y U_y) + C^y U_y + G^y P - \nu K^y U_y + S_y^{ib,c} - \nu S_y^{ib,\nu} = 0.$$

Here $P \in \mathbb{R}^E$ is the discrete pressure, $U_x \in \mathbb{R}^{E_x}$ and $U_y \in \mathbb{R}^{E_y}$ are the discrete components of the velocity vector; $S_x^{ib,c} \in \mathbb{R}^{E_x}$, $S_x^{ib,\nu} \in \mathbb{R}^{E_x}$, $S_y^{ib,c} \in \mathbb{R}^{E_y}$, $S_y^{ib,\nu} \in \mathbb{R}^{E_y}$ are source terms; $\overline{U}^{ib} \in \mathbb{R}^E$ is the mass flux; $D^x \in M(\mathbb{R})_{E \times E_x}$, $D^y \in M(\mathbb{R})_{E \times E_y}$ are the divergence discrete analogues; $K^x \in M(\mathbb{R})_{E_x \times E_x}$ and $K^y \in M(\mathbb{R})_{E_y \times E_y}$ represent the discretization of the diffusive terms; $C^x \in M(\mathbb{R})_{E_x \times E_x}$ and $C^y \in M(\mathbb{R})_{E_y \times E_y}$ represent the discretization of the convective terms; $G^x = -D_x^T$ and $G^y = -D_y^T$ are the gradient discrete analogues.

The time integration of the differential algebraic system (22) is performed with a semi-implicit Euler scheme. Predictor step leads to discrete analogues of the Helmholtz equation for velocities prediction $\widetilde{U}_x$, $\widetilde{U}_y$ at the time $t_{n+1} = (n+1)\Delta t$:

$$\frac{M_x^{n+1}\widetilde{U}_x - M_x^n U_x^n}{\Delta t} + C_x^n U_x^n + S_x^{ib,c,n} - D_x^{T,n} P^n - \nu K_x^{n+1}\widetilde{U}_x - \nu S_x^{ib,\nu,n+1} = 0, \tag{23}$$
$$\frac{M_y^{n+1}\widetilde{U}_y - M_y^n U_y^n}{\Delta t} + C_y^n U_y^n + S_y^{ib,c,n} - D_y^{T,n} P^n - \nu K_y^{n+1}\widetilde{U}_y - \nu S_y^{ib,\nu,n+1} = 0.$$

Here Δt is the constant time discretization step. Corrector step leads to the following discrete analogue of Poisson equation for $\Phi = \Delta t(P^{n+1} - P^n)$:

$$A^{n+1}\Phi = D_x^{n+1}\widetilde{U}_x + D_y^{n+1}\widetilde{U}_y + \overline{U}^{ib,n+1}, \tag{24}$$

$A = -D^x(M^x)^{-1}(D^x)^T - D^y(M^y)^{-1}(M^y)^T$, $A \in M(\mathbb{R})_{E \times E}$. Then flow variables at the time point t_{n+1} are computed by the following formulae:

$$U_x^{n+1} = \widetilde{U}_x + (M_x^{n+1})^{-1} D_x^{T,n+1}\Phi,\ U_y^{n+1} = \widetilde{U}_y + (M_y^{n+1})^{-1} D_y^{T,n+1}\Phi,\ P^{n+1} = \frac{\Phi}{\Delta t} + P^n. \tag{25}$$

Linear systems (23), (24) are solved using the BiCGStab method with the ILU- and multigrid [14] preconditioning. The optimal parameters of the multigrid preconditioner were chosen using the original algorithm for the solver cost-coefficient estimation [15].

5 NUMERICAL EXPERIMENTS

Vortex Element Method implemented in POLARA software package [12] allows to simulate flow-induced vibrations of the airfoil. The computational cost of the simulation process is sufficiently small: time of computations in sequential mode and in parallel mode for 200 second of physical time is shown in table 1 for different values of Sh_ω value. All the computations were performed on cluster with Intel Core i7 2,4 GHz processors.

Table 1: Computational time (in hours) for vortex element method

Sh_ω		1 CPU	2 CPU	4 CPU	8 CPU	16 CPU
0.17	(no resonance)	41.3	22.6	12.0	7.1	4.7
0.21	(max amplitude)	63.4	34.7	17.9	10.1	6.6
0.24	(close to resonance)	45.3	25.4	13.3	7.6	4.8

About 80 computations have been produced for different values of the dimensionless frequency and the unsteady process have been simulated. At the initial time there were still flow and the airfoil in equilibrium position. Time step Δt was equal to 0.01, number of panels which approximates the airfoil $N_p = 200$. Then the velocity of the incident flow became greater; at time moment $t = 1.0$ (after 100 time steps) it was equal to $V_\infty = 3.0$ and then remained constant. After the transient mode airfoil's oscillation in all cases became close to periodical, their amplitudes dependency on the natural frequency Sh_ω is shown on fig. 4, *a* (dots connected by line).

The fig. 4, *a* shows that there is a sharp increase in the amplitude of oscillations at $\mathrm{Sh}_\omega \approx 0.198$. It's well known that there is hysteresis-type phenomenon [16] and in order to simulate it the following computations were performed: from $t = 0$ to $t = 100$ (10 000 time steps) Sh_ω was equal to 0.21; at this time the oscillations become steady with amplitude $A/D \approx 0.47$, then the constraint's elasticity coefficient was changed abruptly to the values which correspond to Sh_ω from 0.178 to 0.198 with step 0.00025. In each case after the transient mode new steady oscillations were generated, and their amplitudes are shown on fig. 4, *b* (dots connected by solid line).

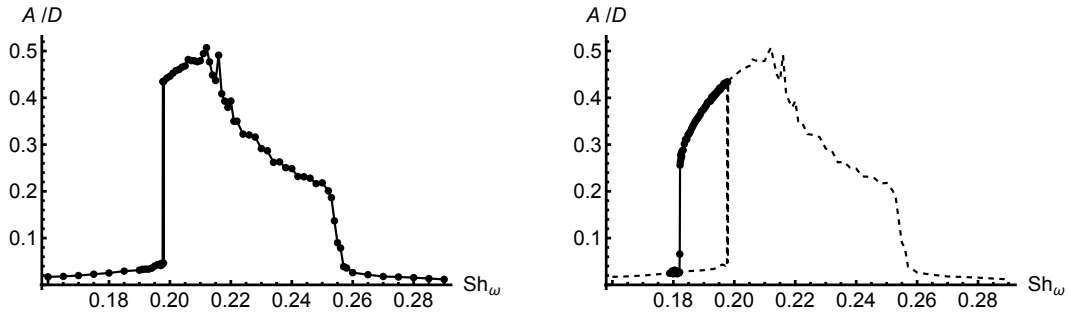

a *b*

Figure 4: Maximum amplitude of the circular airfoil oscillations simulated using vortex element method: *a* – airfoil's initial state id equilibrium position, *b* — airfoil's initial state is close to resonance oscillations

The obtained results for maximum amplitude of oscillation, the resonance frequency and hysteresis properties are in good agreement with the results given in [16, 17].

When using the LS-STAG method number of computations have been performed on non-uniform grid 272×292 with time discretization step $\Delta t = 0.0001$. The maximum amplitudes of oscillations dependency on the Strouhal number Sh_ω is shown on fig. 5.

Computational results are in good qualitative agreement with the previous studies [17]. Maximum amplitude is about $0.4D$ and it occurs when the natural frequency of the system St_ω is close to the Strouhal number, calculated for a fixed airfoil $\mathrm{St} \approx 0.24$ [6].

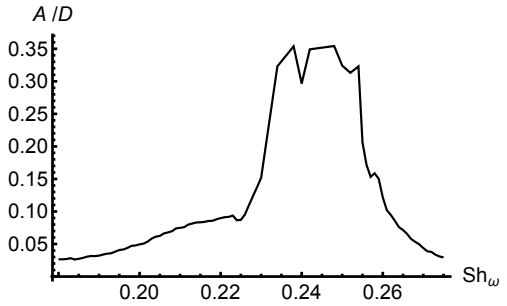

Figure 5: Maximum amplitude of the circular airfoil oscillations at Re = 1000 simulated using the LS-STAG method

The original program package developed by the authors requires approximately 250 hours to simulate 200 seconds of unsteady airfoil's oscillations at resonance mode and about 180 hours at non-resonance mode. In order to obtain more accurate results we need more detailed mesh, but the computational cost of the simulation for such mesh will be extremely high because the program package operates in sequential mode. Its parallelization and acceleration is very important but non-trivial problem.

6 CONCLUSIONS

Two different approaches to numerical simulation of flow-induced vibrations of the airfoil in incompressible flow are considered. The first approach is based on the meshless lagrangian Vortex Element Method while the second one corresponds to the LS-STAG immersed boundary method. Software packages are developed for the numerical simulation of the airfoils' motion in the flow by using the mentioned methods and their modifications. The model problem of wind resonance of the circular airfoil simulation is considered. Both methods allows to obtain satisfactory results; Vortex Element Method seems to be more accurate and it need approximately a fourth of time which the LS-STAG method need for unsteady oscillations simulation. Nevertheless, LS-STAG method seems to be useful in practice for high-Reynolds flows simulation because it allows to implement arbitrary turbulence model while there are no modifications for Vortex Element Method which allows to solve Navier — Stokes equations using RANS, LES or DES approaches.

7 ACKNOWLEGEMENTS

The work was partially supported by Russian Federation President Grants for young scientists [proj. MK-3705.2014.8, MK-5357.2015.8].

REFERENCES

[1] Lifanov, I.K., Belotserkovskii, S.M. *Methods of Discrete Vortices.* CRC Press, 1993.

[2] Cottet, G.-H., Koumoutsakos, P.D. *Vortex Methods: Theory and Practice.* CUP, 2008.

[3] Dynnikova, G.Ya. Lagrange method for Navier — Stokes equations solving. *Doklady Akademii Nauk.* (2004) **399**: 42–46.

[4] Marchevsky, I.K. and Moreva, V.S. Vortex Element Method for 2D Flow Simulation with Tangent Velocity Components on Airfoil Surface. *ECCOMAS 2012 — European Congr. on Comp. Meth. in Appl. Sc. and Eng., e-Book.* (2012) 5952–5965.

[5] Mittal, R. and Iaccarino, G. Immersed boundary methods. *Annu. Rev. Fluid Mech.* (2005) **37**: 239–261.

[6] Cheny, Y. and Botella, O. The LS-STAG method: A new immersed boundary/level-set method for the computation of incompressible viscous flows in complex moving geometries with good conservation properties. *J. Comp. Phys.* (2010) **229**:1043–1076.

[7] Kempka, S.N., Glass, M.W., Peery, J.S. and Strickland, J.H. Accuracy Considerations for Implementing Velocity Boundary Conditions in Vorticity Formulations. *SANDIA Report SAND96-0583* (1996)

[8] Kuzmina, K.S. and Marchevsky, I.K. On Numerical Schemes in 2D Vortex Element Method for Flow Simulation Around Moving and Deformable Airfoils. *Advanced Prob. in Mech. (APM 2014): Proc. of the XLII Summer School-Conf.* (2014) 335–344.

[9] Andronov, P.R., Guvernyuk, S.V. and Dynnikova, G.Ya. *Vortex methods for unsteady hydrodynamical forces calculation.* Moscow University Press, 2006. [in Russian]

[10] Dynnikova, G.Ya. Fast technique for solving the N-body problem in flow simulation by vortex methods. *Comp. Math. and Math. Phys.* (2009) **49**: 1389–1396.

[11] Kuzmina, K.S. and Marchevsky, I.K. Estimation of computational complexity of the fast numerical algorithm for calculating vortex influence in the vortex element method. *Science and Education.* (2013) **10**: 399–414. [in Russian]

[12] Marchevsky, I.K. and Moreva, V.S. High-Efficiency POLARA Program for Airfoil Aerodynamic Characteristics Calculation Using Vortex Elements Method. *ICVFM2010 – Int. conf. on vortex flow and vortex methods.* (2010) 10–15.

[13] Osher, S. and Fedkiw, R.P. *Level set methods and dynamic implicit surfaces.* Springer, (2003).

[14] Wesseling, P. *An introduction to multigrid methods.* John Willey & Sons Ltd., (1991).

[15] Marchevsky, I.K. and Puzikova, V.V. OpenFOAM iterative methods efficiency analysis for linear systems solving. *Proceedings of the Institute for System Programming of RAS.* (2013) **24**: 71–86. [in Russian]

[16] Klamo, J.T., Leonard, A. and Roshko, A. The effects of damping on the amplitude and frequency response of a freely vibrating cylinder in cross-flow. *J. of Fluids and Struct.* (2006) **22**: 845–856.

[17] Klamo, J.T., Leonard, A. and Roshko, A. On the maximum amplitude for a freely vibrating cylinder in cross flow. *J. of Fluids and Struct.* (2005) **21**: 429–434.